Electronic Supplementary Material (ESI) for Soft Matter

On the Alignment of a Cylindrical Block Copolymer: A time-resolved and 3-Dimensional SFM Study

Clemens Liedel [1], Markus Hund [2], Violetta Olszowka [2], and Alexander Böker [1, 3]*

[1] Lehrstuhl für Makromolekulare Materialien und Oberflächen, RWTH Aachen University and DWI an der RWTH Aachen e.V., D-52056 Aachen, Germany

[2] Physikalische Chemie II, Universität Bayreuth, D-95440 Bayreuth, Germany

[3] JARA-FIT, RWTH Aachen University

[*] Corresponding author: boeker@dwi.rwth-aachen.de (A.B.)

Supporting Information

Initial Polymer Structure:

Figure S1 shows the $S_{16}V_{21}T_{63}^{140}$ polymer structure after 9.5 min of $CHCl_3$ annealing. Darker lines in between brighter ones denote to a mainly cylindrical structure.

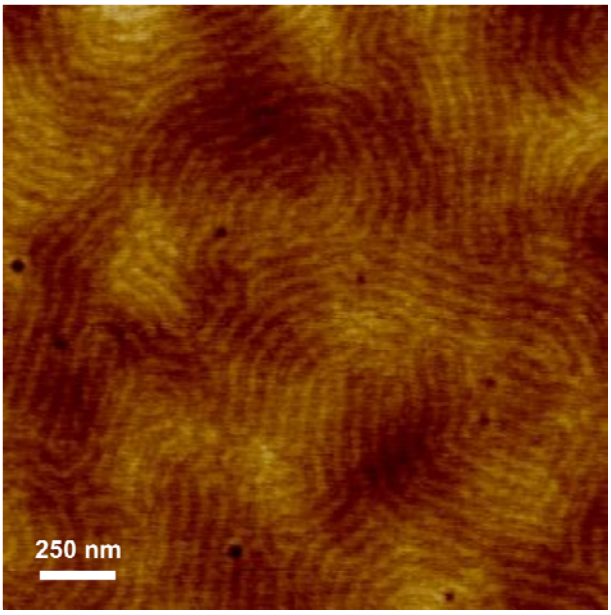

Figure S1: *AFM topographic image (Δz = 10 nm) of a $S_{16}V_{21}T_{63}^{140}$ film after 9.5 min of $CHCl_3$ annealing.*

Chloroform vapor annealing

The interaction parameters χ between the individual homopolymer blocks and the solvent are $\chi_{PS/CHCl3}$ = 0.35, $\chi_{P2VP/CHCl3}$ = 0.38 and $\chi_{P\mathit{t}BMA/CHCl3}$ = 0.40 like derived from the Hildebrand solubility parameters. During chloroform vapor annealing, all of the homopolymer blocks swell to a large extent. PS reaches the 3.5-fold, P2VP the 4.2-fold and P*t*BMA the 3.45-fold of its volume. It could also be proven experimentally that in highly diluted systems, χ conforms to the above mentioned values.[1] As the $S_{16}V_{21}T_{63}^{140}$ films swell to a large extent, the solvent can be seen as nearly unselective.

QIS-SFM E-field annealing:

The PC-controlled process equipment for solvent vapor annealing is based on a setup described in ref. [2] (see page 107 for a 3D CAD model). The manually operated closure device (including sealing device) used in ref. [2-4] was replaced by a newly developed and automatically operated reaction chamber for opening, closing and active sealing.[5]

The annealing process included the following steps: After SFM image acquisition (3 µm x 3 µm, 1024 x 1024 pixels), the tip was withdrawn (1 mm) using the SFM software (NanoScope®, "Withdraw" command). A further separation of tip and sample (6.4 mm) was performed using a self-developed C++ NanoScript™ application. After automatic closure of the chamber, the reactor chamber was automatically sealed hermetically. A self-developed LabVIEW-application (National Instruments, Austin, TX, USA) basically controlled the following devices: Two mass flow controller (MFCs), a mass flow meter (MFM), a voltage power supply and a relay. The following steps were performed automatically: 1) flushing with argon gas; 2) applying an electric field and set a flow of 56 sccm of chloroform vapor; 3) drying the sample surface with pure argon gas (with applied electric field), and finally the grounding of the sample electrodes to the SFM ground pin. The details of the PC-controlled reaction chamber and a fully automated QIS-SFM system featuring a synchronization of data acquisition and sample treatment steps (including sample spot tracking) are described elsewhere.[5]

After opening the chamber automatically, the SFM scanner was approached (6.4 mm) using a NanoScript™-application and engaged with the "Engage" command of the NanoScope® software. This procedure was repeated several times. Thereby the SFM tip could easily and reliably be re-positioned on a specific sample spot. The annealing process is described in detail elsewhere[3, 4]. The total acquisition time of the raw data set is dominated by the total time to anneal and dry the sample.

QIS-SFM nanotomography:

The process was executed as follows: after taking an SFM image (3 μm x 3 μm, 1024 x 1024 pixels), the SFM head was withdrawn using the "Withdraw" command of the NanoScope® software. A further separation of tip and sample was performed with a NanoScript™ applicaton (4.8 mm). The reactor chamber was closed manually and an automated low pressure plasma treatment step was performed using a self-developed LabVIEW application in order to reach reproducible process steps. This included a "soft" step-wise evacuation of the reaction chamber, followed by an automatic process pressure (5 mbar, atmospheric air), ignition and sustaining the plasma for the intended etch time, and the gently venting of the reaction chamber. After opening the chamber manually, the scanner was approached using NanoScript™ followed by an "Engage" command. This process is described in detail elsewhere.[6-8]

The total acquisition time of the raw data set is dominated by the total time to scan the SFM images. The treatment time is usually small compared to the time to scan the images (use of non-high speed scanning technology assumed). For the experiment described here, we used successive plasma etching and SFM measurements (22 process steps, from step to step increasing plasma treatment time, and cumulative etching time of 120 s). The wetting layer beneath the core-shell structures cannot be resolved in this manner. This can be explained by a chemical cross-linking process of the polymers, as especially PS and P2VP tend to cross-link in the presence of free electrons.[9, 10]

Post-processing of the images taken during E-field annealing:

We use median leveling technique (provided with GWYDDION[11] software) in order to analyze small features: Therefore the topography images are median filtered using a large kernel, and the result is subtracted from the original image treated as a background. Only features smaller than approximately the kernel size will be kept.

In a second step, the images were contrast enhanced. The remaining drift between the images was calculated and compensated by rigid registration (see Supporting Info in ref. [7] for details). Cutouts of the images were performed to provide a series of images at exactly the same spot of the sample.

Post-processing of the nanotomographic image series:

For a 3D reconstruction the thickness of the removed layer with prolonged cumulative etching time is crucial, because it determines from which 'depth' the topographic data (with corresponding phase) was detected. Therefore care was taken to investigate the etching behavior in detail using a calibration sample which was equally prepared as the sample taken to perform the nanotomographic experiment. From quasi *in-situ* SFM calibration data sets the film thickness between substrate (the polymer was removed by a scalpel) and polymer surface versus the cumulative etch time was evaluated. We used the same etching protocol as in the following nanotomographic examination. This measure enables us to detect even weak non-linear etch behavior due to the complex sample composition.

We calculated an etch-time dependent ablation function *a(t)*. For details about the ablation function see the following sections. Using this function we calculated the 3D coordinates (voxelization) of the material property (phase information). The generated 3D raw data set was directly loaded into commercial 3D software (AMIRA from Visage Imaging Inc.) and further processed. The used general voxelization algorithm is capable to take into account non-linear etch behavior, the evaluation details and further 3D image processing steps. Further details can be found in ref. [7].

Etching behavior of $S_{16}V_{21}T_{63}^{140}$ polymer films:

For SFM nanotomography, it is crucial to study the thickness dependence in detail in order to avoid errors in the calculation of the 3D reconstruction (see below). Therefore we studied the etching behavior of $S_{16}V_{21}T_{63}^{140}$ using a calibration sample which was prepared exactly in the

same way as the sample taken to perform the nanotomography experiment. We found a slightly non-linear etching behavior (Figure S2). We note that in a generalized voxelization procedure the term $(E_i \cdot t_i)$ (see ref. [7], Supporting Information, p. "V") is replaced by the function $a(t_i)$ so that the 3D matrix holding the physical values is corrected by

$$H[row][col][i] = H[row][col][i] + a(t_i).$$

We note that we use a(t) (Figure S2) as a phenomenological function. The details of the etch behavior were not studied here in detail and go beyond the scope of this paper. Roughly speaking in regime I the top layer of the sample covered with a P*t*BMA matrix material is removed. In regime II the complex core-shell structures are removed, and in regime III the sample surface roughness increases (increased data scatter).

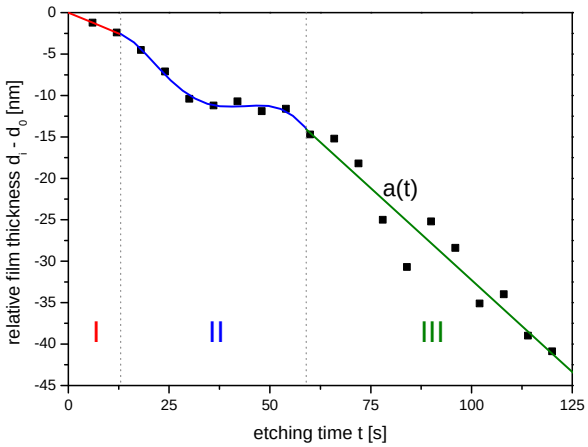

Figure S2: *Relative film thickness of the removed material ($d_i - d_0$) plotted as a function of the cumulative etching time with fitted ablation function a(t). The nonlinear etching behavior is divided into three regimes I, II, and III. The film thickness d_0 denotes the film thickness of the unetched sample and d_i the film thickness after process step i. Regime I ($t \leq 13s$): $-0.2 \cdot t$, regime II ($13s < t \leq 59s$): $-16.3 + 3.02854 \cdot t - 0.21845 \cdot t^2 + 0.006015 \cdot t^3 - 7.07754 \cdot 10^{-5} \cdot t^4 + 2.88527 \cdot 10^{-7} \cdot t^5$, and regime III ($59s < t \leq 180s$): $12.12273 - 0.44394 \cdot t$.*

References

1. H. Elbs, Ph.D. Thesis, Universität Bayreuth, Germany, 2001.
2. V. Olszowka, in *Physikalische Chemie 2*, Ph.D. Thesis, Universität Bayreuth, Germany, Bayreuth, 2007.
3. V. Olszowka, M. Hund, V. Kuntermann, S. Scherdel, L. Tsarkova, A. Böker and G. Krausch, *Soft Matter*, 2006, **2**, 1089-1094.
4. V. Olszowka, M. Hund, V. Kuntermann, S. Scherdel, L. Tsarkova and A. Böker, *ACS Nano*, 2009, **3**, 1091-1096.
5. M. Hund, V. Olszowka, H. Krejtschi and F. Fischer, *Patent Application Publication*, DE 10 2010 015 966 A1, 2011.
6. M. Hund and H. Herold, *Rev Sci Instrum*, 2007, **78**, 063703.
7. A. Sperschneider, M. Hund, H. G. Schoberth, F. H. Schacher, L. Tsarkova, A. H. E. Müller and A. Böker, *ACS Nano*, 2010, **4**, 5609-5616.
8. M. Hund and H. Herold, *Ger. Pat.*, 10 2004 043 191 B4, 24 May 2006 and *US Pat.*, 7 934 417, 3 May 2011.
9. R. Glass, M. Arnold, J. Blümmel, A. Küller, M. Möller and J. P. Spatz, *Advanced Functional Materials*, 2003, **13**, 569-575.
10. E. H. Lee, G. R. Rao and L. K. Mansur, *Materials Science Forum*, 1997, **248**, 135-146.
11. *Gwyddion - Free SPM data analysis software. http://gwyddion.net/*.